ANALYZING PYROXENE CRYSTALS TO DETERMINE CRYSTALLIZATION TRENDS IN NORTHWEST AFRICA 11788 . B. Acevedo[1] and K. M. O'Sullivan[2], Department of Geological Sciences, California State University Bakersfield, Bakersfield, CA 93311 USA (bacevedo4@csub.edu) (kosullivan@csub.edu).

Introduction Samples from the Apollo and Luna missions were the first physical evidence collected that gave insights into the processes that formed the Moon. The revolutionary findings discovered from analyzing these samples led to the development of what is known as the Lunar Magma Ocean model (LMO) [e.g. 1-3]. Once LMO crystallization occurred, lunar lithologies began to differentiate, forming the three layers of the LMO: an outer crust made up of ferroan anorthosites (FAN), a mantle comprising of Mg- and Fe-rich silicate minerals, and a small and dense core [1]. LMO models describe a global residual melt rich in incompatible elements.

Due to the presence of KREEP within many mission samples (with the exception of Apollo 12 and Luna 24) [1,3]. The nature and extent of the KREEP layer remains enigmatic to this day.

Lunar meteorites serve as a great addition to lunar samples, since they provide a random sampling of the Moon's surface [1-7], and are not limited to the Apollo and Luna mission sites [1]. Further, geochemical analysis shows ferroan anorthosites, Mg-suite rocks, and KREEP lithologies appear in different ratios in meteorites compared to those in returned mission samples [1,3]. Therefore, meteorites can provide more insight into the geological history of the Moon [2,4,7]. For example, it has been shown that Apollo samples do not show the homogeneity of lunar lithologies implied in the LMO [3].

Here we present data from lunar feldspathic meteorite Northwest Africa 11788. Adding petrological data to the already-existing database of lunar meteorites will be of great use in setting better constraints on the current LMO model [6], such as global distribution of lunar lithologies [7]. Meteorites are key for calibrating data collected from remote sensing techniques [4] and will aid in future missions to the Moon.

We focus on analyzing pyroxene crystals as they can record the crystallization history of a rock, allowing us to better understand the geological history of the moon. In this study we interpret the relationships of major elements within the core and rims of pyroxene.

Methods: *Petrography*. Photomosaics of thin sections were constructed by capturing images in plane and cross polarized light on a petrographic microscope and stitching them together using *Adobe Photoshop*. The photomosaics were then laid over each other on iPad app *Procreate* to help navigate and label points in thin sections during use of the microprobe at UCLA.

Pyroxene was targeted within rock fragments with emphasis on identifying and analyzing zoned pyroxene.

Quantitative Mineral Analysis. Quantitative mineral data and backscattered electron (BSE) images were obtained using a *JEOL JXA-8200 SuperProbe* electron microprobe (EMP) at the University of California Los Angeles (UCLA) electron microprobe facility. EMP points were obtained with a 15 kV accelerating voltage, a beam current of 10 – 20 nA, and a focused electron beam of 1 μm in diameter.

Results: *Petrography*. Within NWA 11788, crystals of olivine, plagioclase, pyroxene, ilmenite and metals are present. Fig. 1 shows example clasts that were targeted for chemical analysis. Dark areas in Fig. 1 are plagioclase while the mid-light grey is pyroxene and olivine. Small white areas are metals. Both clasts show distinct crystals of felsic materials mixed with mafic ones within the same rock fragment. Both clasts have about ~30% plagioclase and ~70% of pyroxene present. Pyroxene is zoned in each clast. The plagioclase in clast 10 (Fig. 1b) seems to have more of a linear appearance as opposed to the more blocky appearance seen in clast 8 (Fig. 1a). Metal pieces are relatively larger and less broken up in clast 8 as opposed to clast 10. Pyroxene surrounds the majority of the plagioclase in both clasts and tends to be zoned. Both rock fragments are heavily fractured.

A total of 155 crystals were analyzed with 253 points in 11 clasts. Focus was placed on targeting pyroxene within rock fragments and zoning within pyroxene crystals. For example, a total of 13 and 11 crystals were analyzed in clasts 8 and 10, respectively [Fig. 2]. 3 pyroxenes and 10 plagioclase crystals were analyzed in clast 8. 4 pyroxenes, 1 ilmenite, 1 olivine, and 5 plagioclase crystals were analyzed in clast 10.

Quantitative mineral analysis. Figure 2a shows the relationship of Fe# [Fe/(Fe+Mg)] relative to Ti# [Ti/(Ti+Al+Cr)] in pyroxene. Figure 2b shows Fe# [Fe/(Fe+Mg)] relative to atomic Al/Ti in pyroxene. Fe# of pyroxenes within clasts and matrix range from 0.466 to 0.994 with cores and rims ranging from 0.466 to 0.986 and 0.470 to 0.994, respectively (Fig. 2a,b). The Ti# ranges from 0.042 to 0.618 with cores and rims ranging from 0.042 to 0.560 and 0.086 to 0.618, respectively (Fig 2a). Atomic Al/Ti ranges from 0.786 to 13.004 for cores and 0.619 to 7.080 for rims (Fig 2b). Overall, Al/Ti content decreases as Fe# increases.

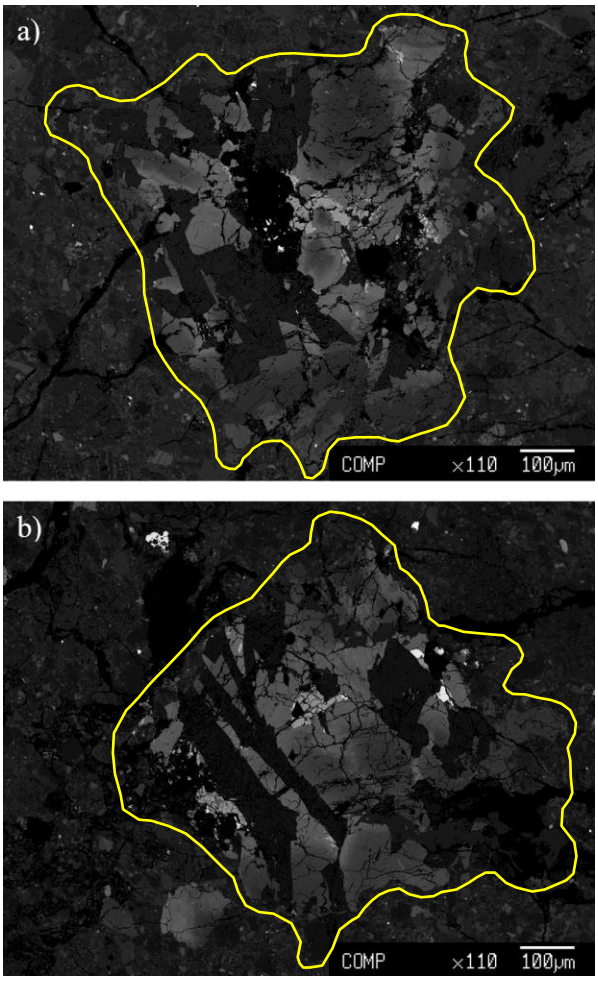

Figure 1. *BSE images of a) clast 8 and b) clast 10 outlined in yellow. Both rock fragments show a mixture of plagioclase (dark areas) with zoned pyroxene and some olivine.*

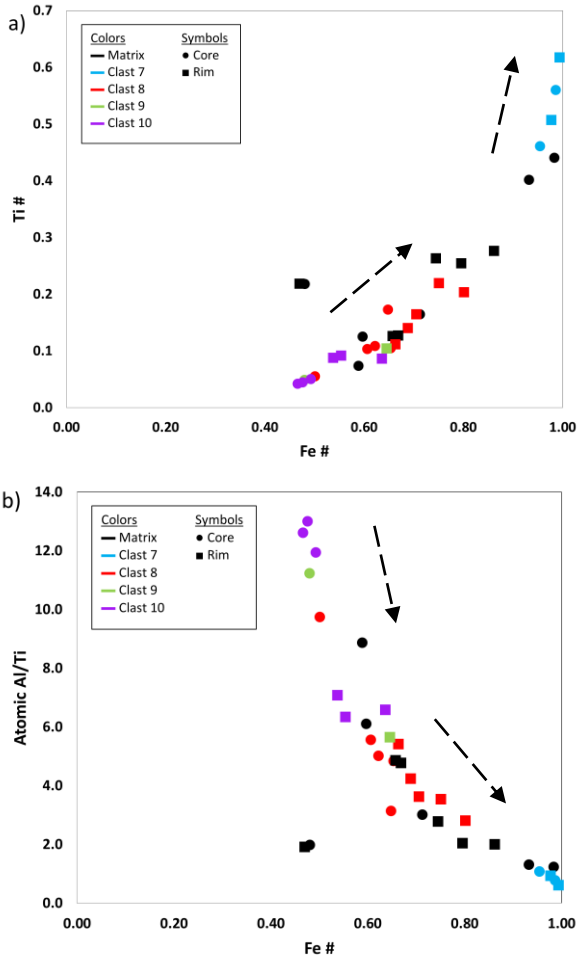

Figure 2. *Major element trends in pyroxene crystals. Circles are pyroxene cores and squares are rims. Black points represent crystals located in the matrix of the thin section and color points represent crystals located within individual rock fragments. Arrows indicate direction of crystallization.*

Discussion: Pyroxene core and rim values record different stages of crystallization. This gives us a rich set of crystals to analyze. As Fe# increases, so does the Ti# [Fig. 2a], indicating a typical trend of fractionation [8,9]. The steep and 45 degree slope of crystallization trend on Figure 2a indicates that there is co-crystallization with chromite and ulvöspinel and no co-crystallization with ilmenite [9].

The downward trend seen in Fig. 2b is consistent with co-crystallization of plagioclase and pyroxene. The negative slope represents a decrease in Mg and Al as crystallization continues, indicating crystallization of both pyroxene and plagioclase. As Al was removed from the melt, the ratio of Al/Ti began to decrease. Trends in Fig. 2b indicate that ilmenite was not co-crystallizing with plagioclase and pyroxene.

Analyzing major elements within pyroxene crystals gives a better understanding of elemental partitioning during crystallization of parental melts, further constraining the lithologies predicted in LMO models.

Future Work: Further EMP analyses of additional clasts is underway. Trace element data using Inductively Coupled Plasma Mass Spectrometry will be presented at LPSC 53.

References:[1] Gross J. et al. (2020) *JGR, 125*, e2019JE006225. [2] Russell S. S. et al. (2014) *Phil. Trans. R. Soc.*, A372. [3] Gross J. et al. (2014) *Earth and Planet. Sci. Letters, 388*, 318-328. [4] Joy K. et al. (2010) *Meteoritics & Planet. Sci., 45*, 917-946. [5] Treiman A. H. and Gross J. (2015) *American Mineralogist, 100*, 414-426. [6] Kent J. J. et al. (2017) *Meteoritics & Planet. Sci., 52*, 1916-1940. [7] Zeng X. et al. (2018) *Meteoritics & Planet. Sci., 53*, 1030-1050. [8] Curran N. M. et al. (2019) *Meteoritics & Planet. Sci., 54*, 1401-1430. [9] Snape J. et al. (2014) *Meteoritics & Planet. Sci., 49*, 842-871.